Influence of production variables and starting material on charcoal stable isotopic and molecular characteristics

Authors and affiliations: P. L. Ascough[1*], M. I. Bird[1], P. Wormald[2], C. E. Snape[3], D. Apperley[4]

[1]Department of Geography and Geoscience, University of St. Andrews, Irvine Building, St. Andrews, Fife, KY16 9AL, UK.

School of Chemistry, University of St Andrews, Purdie Building, St. Andrews, Fife, KY16 9ST UK.

[3]School of Chemical, Environmental and Mining Engineering, University of Nottingham, NG7 2RD, UK

[4]EPSRC Solid-State NMR Service, Industrial Research Laboratories, University of Durham, South Road, DH1 3LE, Durham, UK

[*]Corresponding author. Tel.: +44 1334463936; fax: +44 1334 463949. E-mail: pla1@st-andrews.ac.uk (P. L. Ascough).

NB: This is a revised version of the manuscript W5637. Submission date 07/03/2008

Abstract

We present a systematic study on the effect of starting species, gas composition, temperature, particle size and duration of heating upon the molecular and stable isotope composition of high density (mangrove) and low density (pine) wood. In both pine and mangrove, charcoal was depleted in $\delta^{13}C$ relative to the starting wood by up to 1.6‰ and 0.8‰ respectively. This is attributed predominantly to the progressive loss of isotopically heavier polysaccharides, and kinetic effects of aromatization during heating. However, the pattern of $\delta^{13}C$ change was dependant upon both starting species and atmosphere, with different structural changes associated with charcoal production from each wood type elucidated by Solid State ^{13}C Nuclear Magnetic Resonance Spectroscopy. These are particularly evident at lower temperatures, where variation in the oxygen content of the production atmosphere results in differences in the thermal degradation of cellulose and lignin. It is concluded that production of charcoal from separate species in identical conditions, or from a single sample exposed to different production variables, can result in significantly different $\delta^{13}C$ of the resulting material, relative to the initial wood. These results have implications for the use of charcoal isotope composition to infer past environmental change.

1 INTRODUCTION

Charcoal is formed from the incomplete combustion of biomass in reducing conditions (Chaloner, 1989). This results in material with typically a high (60-90%) carbon content, a proportion of which exists in highly stable condensed aromatic molecular configurations (Eckmeier *et al*., 2007). Consequently, charcoal forms part of the environmentally recalcitrant "black carbon" continuum (Czimczik *et al*., 2005), with some material not re-oxidized to CO_2 over geological timescales (Levine, 1991). In addition, charcoal is present in many modern soils and sediments, comprising ~30% of the total organic carbon in some Australian and US soils (Skjemstad *et al*., 1996; 2002). This abundance and apparent environmental recalcitrance makes charcoal a crucial source of palaeoenvironmental and archaeological proxy data, used to reconstruct records of fire history, human societal and climate change (Carcaillet *et al*., 2002, Gavin *et al*., 2002; Goebel *et al*., 2003).

In living plants, distinct differences in stable carbon isotopic composition ($\delta^{13}C$) arise between those using the Calvin-Benson (or C_3) photosynthetic pathway, (typical $\delta^{13}C$ of –20 to -30‰), and those using the Hatch-Slack (or C_4) pathway (typical $\delta^{13}C$ of –10 to -15‰) (Ehrlinger *et al*., 1997; 2002). Plant $\delta^{13}C$ is strongly influenced by the ratio of intercellular to ambient CO_2, and is modulated by factors of soil moisture status, relative humidity, irradiance and temperature (McCarroll and Loader, 2004). Therefore, $\delta^{13}C$ measurements are used to infer variations in climatic conditions during plant growth (e.g. Robertson *et al*., 1997). As charcoal is derived from plant biomass, charcoal carbon isotopic ($\delta^{13}C$) measurements are commonly made in palaeoenvironmental reconstruction (e.g. Clark *et al*., 2001; Pessenda *et al*., 2005;

Ferrio *et al*., 2005; Hall *et al*., 2008), under the assumption that isotopic fractionation induced during charcoal formation is absent (Marino and DeNiro 1987, Novakov *et al*., 1994). However, growing evidence suggests an offset in $\delta^{13}C$ between the initial plant tissues and charcoal. Following heating over 100°C, $\delta^{13}C$ values are elevated by up to 3.5‰ in bulk soil organic carbon, 2.0‰ in carbonized vegetation, 1.5‰ in plant propagules and 1.9‰ in wood (Cachier *et al*., 1985; Turekian *et al*., 1998; Werts and Jahren, 2007; Poole *et al*., 2002; Krull *et al*., 2003). In other work however, decreases of up to 1.8‰ have been observed in wood charcoal following heating up to 800°C (Jones *et al*, 1993, Czimczik *et al*., 2002; Turney *et al*., 2006). Therefore, although available evidence suggests isotopic changes during charcoal production, both the sign and magnitude of fractionation effects is highly variable.

One explanation for the observed $\delta^{13}C$ changes is the differential thermal degradation of isotopically distinct wood components. Wood is typically comprised of 36-40% cellulose, 25-30% hemi-cellulose, c.28% lignin and a range of extractives (Sjöström, 1993; Verheydan *et al*., 2005; Gleixner *et al*., 1993). These are isotopically distinct; cellulose $\delta^{13}C$ is on average ~1‰ greater than whole wood, lignin $\delta^{13}C$ is on average ~2‰ lower than whole wood (Maunu *et al*., 2002; Benner *et al*., 1987; Loader *et al*., 2003). Cellulose degrades rapidly at 250-400°C and lignin more slowly at 200-720ºC (Williams and Besler, 1996; Xiao *et al*., 2001). Therefore, changes in the proportion of different components following biomass heating could result in $\delta^{13}C$ variations (e.g. Czimczik *et al*., 2002). Such an effect could also result in species-dependant isotopic changes, as is already observed in the rate of chemical transformations during pyrolysis (exposure to elevated temperatures in the absence of oxygen) (Labbé *et* al., 2006).

Systematic investigation is therefore required, of the effect of factors including starting material and production conditions upon charcoal $\delta^{13}C$. Such an investigation can be usefully combined with examination of molecular structural changes during heating, allowing simultaneous monitoring of isotopic changes and the accompanying thermal degradation of different wood structural components. An effective methodology for such work is provided by Solid State ^{13}C Nuclear Magnetic Resonance Spectroscopy, using cross-polarization magic angle spinning (^{13}C-CP-SSNMR). This technique reveals detail in the structure of lignocellulosic material via the ^{13}C signal intensity and chemical shift. Though for biomass these shifts are often broad and complex, the technique allows differentiation of specific carbon (C) environments, such as within the cellulose glucopyranose ring (Martínez *et al*., 1999). ^{13}C-CP-SSNMR is therefore used to monitor wood structural changes during physical and chemical treatment, including heating (Evans *et al*., 1995; Wormald *et al*., 1996; Baldock and Smernik, 2002). In such studies, the effect of differing thermal stabilities between wood components is apparent, with more significant alteration of signals attributed to cellulose carbons than those of lignin (Inari *et al*., 2007). Characteristic changes include a reduction in intensity in the O-alkyl and di-O-alkyl regions (65-110 ppm) and an increase in aryl and O-aryl C during production of aryl and O-aryl furan-like structures (Baldock and Smernik, 2002). As temperatures increase, the chemical shift values increasingly centre at ~127ppm, typical of condensed aromatic carbon produced in both natural and laboratory-produced charcoals (Czimczik et al 2002; Simpson and Hatcher, 2004).

This study aims to establish and explain structural and isotopic changes between starting material and the resultant charcoal, under different production conditions, for wood from different species. Understanding these processes has important benefits as charcoal is not a homogeneous material, but produced under a wide variety of conditions from different species. Understanding the effect these processes have on isotopic composition and structure feeds directly into the effective use of charcoal isotopic measurements as an accurate source of proxy data.

2 METHODS

2.1 Characterisation of raw materials

Two woods were used in the study; a sample of Scots Pine (*Pinus sylvestris L.*), obtained from Tentsmuir Forest, Fife in November 2005, and a sample of mangrove (*Rhizophora apiculata* Blume), collected in North East Palawan, Philippines, in February 2006. These woods were chosen for their differences in density (0.41 ± 0.05 g/m^3 in the pine sample and 0.88 ±0.03 g/m^3 in the mangrove), and composition, representing a softwood and hardwood, respectively. Bulk lipids were extracted from the woods by accelerated solvent extraction of 1g of ground wood, using 500ml of 2:1 (v/v) dichloromethane/methanol, following which the $\delta^{13}C$ values and carbon weight percent (%C) for the extracts were determined as described below.

It is possible for the $\delta^{13}C$ of raw wood to vary by c.2-3‰ in an individual plant due to variations in internal plant structural and external climatic and growth conditions (Leavitt and Long, 1984; McCarroll and Loader, 2004; Wilson and Grinstead, 1977). Hence, all charcoal was produced from a single, homogenized initial sample from both species, obtained from an individual branch of either wood type. For pine this was the outermost 15 rings of the branch, and for mangrove this was the entire branch cross-section, excluding the bark of the tree in both cases. The wood samples were processed to a larger and a smaller sample size, firstly by cutting to $1cm^3$ cubes, which formed the larger size sample, and then by grinding in a Tema mill for 30 seconds to produce a 1-2mm fraction, which formed the smaller sample size.

2.2 Thermogravimetric analysis

Proximate and isothermal analysis of the two woods was performed using thermogravimetric analysis (TGA) on a SDT Q600 differential thermal analyser. The proximate analysis consisted of equilibration in N_2 at 50ºC, followed by pyrolysis to 1100ºC in a nitrogen atmosphere, while the isothermal technique used a temperature of 525ºC, residence time of 80 minutes and an atmosphere of air (Sima-Ella, *et al.*, 2005). Proximate analysis allowed identification of the temperatures of maximum sample mass loss using the first derivative of the TGA data. Isothermal analysis allowed generation of a carbon burnout profile, to assess the reactivity of the two devolatilized woods during thermal degradation.

2.3 Charcoal production

Charcoal was produced in a controlled-atmosphere rotary furnace (Carbolite) for periods of either 60 or 120 minutes duration with an initial heating rate of 10ºC min^{-1}. Four temperatures were used, between 300-600ºC, covering a range representative of natural fires (e.g. Swift *et al*., 1993), in which significant changes in structure are observed (Williams and Besler, 1996). Temperature was determined via a thermocouple inserted into one of the wood cubes in each run. During production of the first suite of 32 samples the furnace was continuously purged with nitrogen at a constant metered flow rate of 7 l/min. The second sample suite was produced under identical conditions, but with 2% O_2 mixed with the purge gas prior to introduction to the furnace. The above protocols produced a matrix of 64 charcoal samples for analysis.

After the heating interval was complete, the samples were allowed to cool to room temperature (20ºC) under the same gas flow, and the mass loss of the sample was determined by comparison of the pre- and post- charcoal production sample weights. Each charcoal sample was then ground to pass a 500μm sieve before treatment with 0.5M HCl for 24 hours to remove calcitic ash. Following the HCl treatment the samples were neutralized with deionised H_2O and wet-sieved to 63-500μm before drying. The moisture and ash content of the samples was measured by loss on ignition, using the weight change of three replicates for each sample during drying to a constant weight in a muffle furnace at 105ºC for 24 hrs, followed by combustion in air at 1020ºC for 6 hrs, where the measurement precision was ± 0.5%.

2.4 Carbon content and stable isotopic composition

Charcoal samples were air-dried prior to analysis and stored in capped glass vials. The sample $\delta^{13}C$ values and organic carbon (%C) content (by weight percent (%C)) were determined using a Costech elemental analyser (EA) fitted with a zero-blank auto-sampler coupled via a ConFloII to a ThermoFinnegan Delta^{plus} XL using Continuous-Flow Isotope Ratio Mass Spectrometry (CF-IRMS) at the University of St. Andrews Facility for Earth and Environmental Analysis. Duplicate measurements were undertaken for each sample, and each sample run included a mix of samples, laboratory standards and blanks, with three internal standards measured with samples. Precisions (SD) on internal standards were better than ±0.3% (1σ) for %C, and better than ±0.2‰ (1σ) for $\delta^{13}C$. The isotopic values for the samples are reported as per mil (‰) deviations from the VPDB international standard.

2.5 ^{13}C-CP-SSNMR

^{13}C-CP-SSNMR spectra were obtained from samples of i.) Untreated pine and mangrove wood, and ii.) Charcoal produced from 1cm^3 cubes of both species as described above. Spectra were recorded on a 300MHz Varian UnityInova or a 500 MHz Varian Infinityplus spectrometer, operating at a carbon frequency of 75.398 MHz and 125.3 MHz respectively at ambient temperature. The 300 MHz spectra were recorded using a 5mm Chemagnetics Apex probe and the 500MHz spectra using a 4mm Chemagnetics T3 triple channel probe. The rotors in both cases were Zirconium oxide fitted with vespel end caps. Spinning speeds were between 6 and 8 kHz with a CP contact time of 0.2 or 1 ms and a 0.5 or 1ms recycle time. The number of transients varied between 1000 and 5000 and spectra were referenced to tetramethylsilane. The pulse program used was a standard Cross-polarization (CP) sequence with a flip-back pulse.

In ^{13}C-CP-SSNMR, quantitative reliability of the spectra is affected by both overlap between peaks derived from different compounds, such as cellulose and lignin, and the difference in proton spin-lattice relaxation time in the rotating frame ($T_{1\rho}{}^{H}$) of different carbons (Nogueira *et al*., 2004; Blann *et al*., 1981). Therefore, differences in spectral intensity may relate more to differences in cross polarization and $T_{1\rho}$ rates than quantitative differences in the content of specific compounds. For example, carbon atoms remote from protons, (e.g. quaternary carbons) may be underrepresented, due to slower rates of cross polarization (Alemany *et al*., 1983). We have therefore elected to compare only the relative intensity of components in the broader groupings of aliphatic (alkyl and O-alkyl), and aromatic structures. Spectra

were divided into chemical shift regions relating to aliphatic and aromatic structures on the basis of minimum intensity (typically 0-115 and 115-190ppm, respectively). The relative areas were calculated by integration and the proportion of aliphatic and aromatic signal in the spectra was then expressed as relative intensity, as a percentage of total area.

3 RESULTS

3.1 Mass loss, %C content and $\delta^{13}C$

The woods had similar %C content, with the mangrove having a slightly lower $\delta^{13}C$ value than pine. Extracted lipids had higher %C content and a lower $\delta^{13}C$ value than the bulk wood in both species. (Table 1).

Charcoal ash contents were uniformly low (<1%) with insignificant inter-sample variation, while moisture content increased with increasing temperature and duration of heating (Table 2). Proximate TGA analysis (Figure 1) suggests maximum volatile loss from both woods occurred at 300-400ºC, a large proportion of which relates presumably to cellulose decomposition (Li *et al*., 2002; Soares *et al*., 2001). Proximate TGA also indicates that components released as volatiles during heating of pine (maximal release 423ºC) have higher thermal stability than those in mangrove, (maximal release 386ºC). The more rapid burn out profile of mangrove during isothermal TGA (Figure 2) shows higher reactivity in devolatilized mangrove wood.

In all sample groups, charcoal production resulted in a strong, non-linear, temperature dependent mass loss (Table 2), which was greater overall for pine than mangrove. Mass losses are markedly increased (by up to 23%) by charring in 2% O_2, with greater physical degradation (e.g. surface cracking) noted on visual inspection, particularly in samples heated for longer time periods (120 min), and for the smaller (1-2mm) size fraction. This led to near complete decomposition to ash in the smaller mangrove fraction following heating above 500ºC, making it impossible to obtain sufficient material for further analysis.

Charcoal %C content is also strongly correlated with production temperature (Table 3); this increased rapidly to 500ºC, converging on 86.1 ± 1.6%. Mangrove %C increases exceed those in pine for all conditions, and greater overall %C increases are observed during production under N_2, up to 500ºC. Heating duration and particle size appear to have little influence on charcoal %C, with small and inconsistent differences between samples.

The $\delta^{13}C$ of pine charcoal was consistently lower than the starting wood by up to 1.6‰ for all production conditions and particle sizes (Table 4, Figure 3), with an average wood-charcoal offset of -0.9‰. In contrast, although mangrove samples show $\delta^{13}C$ decreases of up to -0.8‰, a number of mangrove charcoal samples have a $\delta^{13}C$ that is within error (±0.2‰) of the wood, and at 300ºC an increase in $\delta^{13}C$ of up to 0.5‰ is observed in some samples (Table 4, Figure 4). In pine, there is no consistent difference in $\delta^{13}C$ between charcoal samples produced in the presence or absence of O_2, whereas in mangrove, samples pyrolysed under N_2 show consistently lower $\delta^{13}C$ values than samples produced under 2% O_2. These differences are greatest in the smaller size fraction where, for example, samples pyrolysed for 120 min in 2% O_2 show an average $\delta^{13}C$ decrease of 0.5‰.

The data provide evidence that charcoal $\delta^{13}C$ values decrease with increasing production temperature. For example, the largest wood-charcoal $\delta^{13}C$ offset for pine (-1.6‰) is at the highest temperature (600ºC), where charcoal $\delta^{13}C$ values are on average 1.2‰ lower than the starting wood, compared to an average 0.7‰ reduction in pine $\delta^{13}C$ following heating at 300ºC. In contrast, size fraction and heating duration

does not appear to exert a consistent effect upon charcoal $\delta^{13}C$ for either of the species.

3.2 3.2. ^{13}C-CP-SSNMR

In the unpyrolysed wood, the ^{13}C-CP-SSNMR spectra are dominated by resonances attributable to cellulose and hemicellulose between 60-105 ppm (Figures 5 and 6, (A) and (A1)). Cellulose contains carbon in six different positions (C1-C6), where the C1 and C4 carbons form the glycosidic bonds linking the polymer, and are seen as a broad signal at ~105ppm (C1) and peaks ~89 and 84ppm (C4) (Atalla and Vanderhart, 1999; Earl *et al*., 1981). Glucopyranose ring carbons (C2-C5) are represented at 72-75ppm, and the C6 carbon (CH_2OH group) give peaks at 62ppm and 65ppm. Hemicelluloses are visible in a shoulder on the C1 peak at ~102ppm (Irbe et al., 2001) and acetyl groups (CH_3COO^-) at 21ppm (Knicker 1996; Mörck and Kringstad, 1985). Lignin is represented by methoxyl groups at 56ppm (Hatcher *et al*., 1989), and phenolic compounds at 110-160ppm. In mangrove, a peak at 153ppm shows etherified carbons of syringyl units, whereas in pine, peaks at 147ppm and 113ppm relate to guaiacyl carbons (Kringstad and Mörck, 1983). The mangrove lignin methoxyl peak is more pronounced, as syringyl is dimethoxylated and guayacil monomethoxylated.

In all samples there is a decreasing range in spectral intensity as temperature increases, due predominantly to the loss of intensity in signals related to cellulose, and a dramatic increase in overall aromaticity (Table 5, Figures 5 and 6). In all cases, the correlation between increasing aromaticity and production temperature most closely fits a second-order polynomial relationship (Figure 7), with r^2 values for the

correlation from 0.91 to 0.99 (P = <0.05). Following heating, there are differences between the spectra, most readily visible at 300ºC, which appear to relate to starting species and production atmosphere.

At 300ºC, when pine is heated in N_2, signal remains at 56ppm and ~147ppm for methyl-ether linkages and aromatic guyacil structures in lignin, and for cellulose at 60-80ppm (Figure 5 (B)). Although the signal for the acetyl groups of hemicelluloses at 21ppm has been lost, a signal around 24ppm indicates aliphatic-C structures that are apparently heat-resistant to 300ºC. After heating under 2% O_2 all cellulose signals are attenuated, leaving only a small contribution at 72-75ppm, indicating more advanced degradation of the cellulose component than observed under N_2 (Figure 5 (B1)). Production of mangrove charcoal at 300ºC under N_2 shows a similar pattern to pine, with again a significant amount of aliphatic-C remaining as a broad, unresolved band at 10-50ppm, and increased relative intensity of the methoxyl peak at 56ppm indicating remaining lignin structures. However, loss of all peaks in the 60-110ppm region shows more complete cellulosic degradation than is observed in pine under N_2. Heating of mangrove under 2% O_2 at 300°C does not appear to result in the increased cellulosic degradation observed in pine, as pyranose rings and glycosidic linkages (removed during heating under N_2), clearly remain intact (Figure 6 (B and B1)).

At 300ºC, a relatively large proportion of the carbons in all samples are present in forms other than condensed aromatic structures, however at higher temperatures, signals coalesce towards a single peak centred on ~127ppm, which has been previously assigned to aromatic ring structures in pyrogenic carbon (Simpson and Hatcher, 2004). As production temperature increases, the width of the aromatic peak

is reduced in all samples, suggesting a decrease in the diversity of structural modifications, which is directly related to formation temperature.

4 DISCUSSION

The results support the interpretation that i.) Charcoal samples can show significantly different (>0.2‰) $\delta^{13}C$ values to that of the starting material, ii.) These values are correlated with structural changes visible in the ^{13}C-CP-SSNMR spectra, and iii.) The magnitude of isotopic and structural changes in charcoal is directly dependent upon the starting material and conditions under which the material was produced.

4.1. Mass loss and %C content

Sample mass loss and %C increases as a function of temperature, as previously established, with lower mass loss in larger particles, as longer volatile transport times allow a greater amount of secondary char-forming reactions (Antal and Varhegyi, 1995, Mok *et al*., 1992; Richard and Antal, 1994). Rapid mass loss at 300-400ºC is largely related to cellulose decomposition, with a corresponding rise in aromaticity and %C as O and H bearing structures such as methoxy-C and carbons in pyranose rings are lost (Table 3, Figures 5 and 6). There is a decreased difference in %C between samples at higher temperatures, due to increasing structural similarities and dominance of aromatic structures.

As softwood lignin content is generally higher than hardwood (Pandey, 1998), higher overall mass losses and slower rates of %C increase in pine are likely to relate to degradation of a larger content of low thermal stability extractives <300ºC (e.g. Fengel and Wegener, 1984; Völker and Rieckmann, 2002), that have a C content 15.8% greater than that of whole wood (Table 1, Figure 1). Under 2% O_2, the higher reactivity of mangrove (evident in the isothermal TGA results; Figure 2), meant near

complete loss of some samples at temperatures >500ºC. Specific wood chemistry may therefore catalyse oxidative degradation reactions, with important implications for palaeo-reconstruction, as at higher temperatures, more reactive wood species may be proportionally under-represented in environmental records.

4.2. $\delta^{13}C$ variations during charcoal formation

Heating under N_2 results in up to 1.6‰ and 0.8‰ reduction in $\delta^{13}C$ of pine and mangrove respectively. These values are comparable with other studies, which show $\delta^{13}C$ reductions of up to 1.6‰ in biomass charred in vacuo (Bird and Gröcke, 1997) and up to 2‰ in wood charcoal formed in both restricted O_2 availability and air (Turney *et al*., 2006). In pine charcoal, although the presence of O-alkyl C at 50-100ppm (from ^{13}C-CP-SSNMR) shows persistence of some cellulosic carbons at 300ºC, the loss of the C1 and C4 of cellulose demonstrates depolymerisation of the molecule by transglycosylation (Inari *et al*., 2007). In contrast, the relative intensity of signal from lignin-derived structures, such as the 56ppm methoxy-C peak is increased in the spectra (Figures 5 and 6; B and B1). The lower $\delta^{13}C$ values at 300ºC seen in pine can therefore be attributed to the faster thermal degradation of isotopically heavier cellulose in pine. Char yields from lignin are generally higher than from cellulose, due to higher carbon content in this compound (Antal *et al*., 2000). As the $\delta^{13}C$ of the respective products following charring of isolated cellulose and lignin (e.g. levoglucosan), is equivalent to that of their precursors (Steinbeiss *et al*., 2006), the reduction in $\delta^{13}C$ during production of pine charcoal may result from a greater contribution of isotopically lighter lignin-derived carbon to the developing charcoal structure. The reduction in $\delta^{13}C$ over 400ºC is unlikely to result from continued

removal of cellulose, as near complete thermal degradation of aliphatic-C has occurred. Instead, kinetic effects may dominate the process, due to preferential formation of ^{12}C-^{12}C bonds during aromatic condensation, resulting in ^{13}C-depleted condensation products (Qian *et al.*, 1992). Molecular structural changes in the samples following heating can be correlated with changes in $\delta^{13}C$. The relationship between aromaticity and production temperature is non-linear (Figure 7), reflecting slower conversion rates to aromatic structures at higher temperatures as the concentration of non-converted alkyl and O-alkyl structures becomes more limited. When the relative intensity of aromatic structures in the ^{13}C-CP-SSNMR spectra is plotted versus $\delta^{13}C$ of sample materials, a strong linear correlation is apparent in pine charcoal produced in both N_2 and 2% O_2, where $r^2 = 0.97$ ($P = 0.002$) and $r^2 = 0.91$, ($P = 0.011$) respectively (Figure 8).

In mangrove, although the largest wood-charcoal $\delta^{13}C$ offsets also occur at the highest temperatures and the ^{13}C-CP-SSNMR spectra show broadly similar structural changes to pine during heating, there is a different relationship between aromaticity and $\delta^{13}C$ at low temperature (300°C; Figure 8). At 300°C there is an increase in some mangrove $\delta^{13}C$ values relative to the starting wood. Following this, mangrove charcoal $\delta^{13}C$ falls, although the reduction relative to the starting wood is smaller than that observed in pine. A contributing factor to initial increased mangrove $\delta^{13}C$ at 300°C may be degradation of extractives above 160°C (Hakkou *et al.*, 2006). In mangrove, these have $\delta^{13}C$ 4.2‰ less than whole wood; whereas in pine, the extractive-wood $\delta^{13}C$ offset is much lower (Table 1).

Another consideration is difference in the relative contribution of isotopically distinct compounds to pine and mangrove charcoal. The conversion of carbohydrates, protein, lipids and lignin to char produces similarities in ultimate structure, for example the characteristic ^{13}C-CP-SSNMR signal at ~120-130ppm is produced by thermal degradation of both lignin and cellulose (Sivonen *et al*., 2002; Wikberg and Maunu, 2004; Soares *et al*., 2001). A higher contribution of C derived from cellulosic structures to the mangrove charcoal developed in the initial stages of production, may therefore explain a lower wood-charcoal δ^{13}C offset in this species. From temperatures of 300°C upwards, it is apparent that δ^{13}C in mangrove follows a similar pattern to that in pine, being strongly correlated with aromaticity, with $r^2 = 0.98$ ($P = 0.008$) and $r^2 = 0.95$ ($P = 0.023$) for heating in N_2 and 2% O_2, respectively (Figure 8). At higher temperatures therefore, it is likely that as progressive aromatization becomes the dominant process, similar reactions occur in charcoal produced from both species, with δ^{13}C depletion during condensation and rearrangement.

In mangrove, δ^{13}C changes in charcoal appear to be further modulated by production atmosphere. Heating of pine under 2% O_2 results in more rapid thermal degradation of both cellulosic and lignin components, and more extensive aromatization than under N_2 (Figure 5). However, this acceleration of degradation does not induce significant δ^{13}C differences relative to production under N_2 (Figure 3, Table 4). In contrast, heating of mangrove under 2% O_2 results in samples in which ^{13}C-CP-SSNMR cellulosic signals at 0-115ppm are better resolved at 300°C, and δ^{13}C values overall are slightly higher than those prepared in N_2 (Figure 4, Figure 6, Table 4). During heating in the presence of O_2, angiosperm lignin has been observed to be more stable than in N_2 alone (Li *et al*., 2002). A greater proportion of the mangrove charcoal

structure may therefore be derived from cellulosic carbon during initial production at lower temperatures under 2% O_2. This offset is then reflected in subsequent alterations following progressive heating at higher temperatures.

Linear prediction of changes during charcoal production is clearly complicated by complexities within the structure of native wood (Antal *et al*., 2000), and features specific to different species have potential to induce large variability. Such features include increased thermal resistance of hemi-cellulose by binding in lignin-carbohydrate complexes, and protection of carbon within phytoliths, which have the potential to induce significant differences in isotopic variation during charcoal formation (Beramendi-Orosco *et al*., 2006, Krull *et al*., 2003) Overall therefore, the results suggest that it is unlikely that charcoal $\delta^{13}C$ can be calculated in every case by simple mass balance from the $\delta^{13}C$ value of initial wood components.

4.3. Implications for palaeoenvironmental reconstruction

The results presented here imply that careful consideration is required when considering the level of precision to which measured $\delta^{13}C$ directly reflects palaeoenvironmental conditions. Clearly, charcoal $\delta^{13}C$ is offset from the initial wood by a varying degree, dependent upon specific wood chemistry and production conditions. For example, the average offset between unheated mangrove and pine wood is -1.4‰, however this reduces to -0.7‰ following heating at 600°C. Modulation of $\delta^{13}C$ changes by production conditions increases the complexity of interpretation in thermally-altered samples, as it is unlikely that conditions have remained identical for every burning event represented within a sedimentary

sequence. It is also important to consider factors such as the reactivity of different plant species, as under certain conditions some woods may be pyrolysed to charcoal while others are entirely degraded and hence will not enter the sedimentary record.

Although $\delta^{13}C$ changes on heating affect comparisons between individual charcoal $\delta^{13}C$, it appears that isotopic signals related to climatic variations during the life of the plant (i.e. within different growth rings) are preserved during charcoal production (Hall *et al*., 2008). The results of this study however suggest that qualitative reconstruction would be affected if a range of different conditions existed during charring within a larger individual sample. This could result from thermal gradients through the material and variable internal transport of O_2 due to cracking at the sample surface.

It has been suggested that correction for an offset in wood and charcoal $\delta^{13}C$ may be possible if definite correlations between $\delta^{13}C$ and production variables could be established (c.f. Turney *et al*., 2006). Such a relationship could also permit reconstruction of production conditions via measurement of charcoal $\delta^{13}C$ (c.f. Werts and Jahren, 2007). However, this study suggests that prediction of $\delta^{13}C$ variation is complicated by the effects of species and production conditions. The inability to retrospectively reconstruct these for all samples in the natural environment limits the precision to which such corrections could be made. For investigations which examine palaeoenvironmental data through isotopic measurements of charcoal-containing sample it is clearly important to consider the effect of heating on $\delta^{13}C$. We therefore recommend that to reliably attribute differences in measured sample isotopic values in physically separate individual samples to palaeoenvironmental factors, a suitable level

of difference is used, larger than the uncertainty introduced by isotopic change in wood during charcoal production. For C_3 plants, an appropriate value would be at least >2‰, as this is the upper limit of wood-charcoal $\delta^{13}C$ offsets observed in this study and therefore avoids interpretative uncertainties introduced by isotopic changes in biomass following heating. Given the wide range of conditions that exist during production of charcoal within different global environmental settings, a further research focus should be analyses and comparisons of an extended series of these variables with respect to charcoal produced under natural conditions. This would enable fuller understanding of the heterogeneity in charcoal present in the palaeoenvironmental record, and further enhance interpretative accuracy based upon measurements of this material.

5 CONCLUSIONS

Exposure to temperatures >300ºC in a reducing environment results in $\delta^{13}C$ depletion in pine and mangrove charcoal of up to 1.6‰ and 0.8‰ respectively. ^{13}C-CP-SSNMR suggests that the most likely cause of this depletion is differential thermal degradation of isotopically distinct compounds during structural rearrangement accompanying charcoal production. The greatest variation in molecular structure and isotopic values is observed at lower temperatures (300ºC), whereas up to 600ºC charcoal structures become increasing similar, consisting of highly aromatic structures represented at ~124-128 ppm, apparently representative of the most stable products of biomass charring. Despite the similarities in ^{13}C-CP-SSNMR spectra at higher temperatures, significant offsets (>0.2‰) in charcoal $\delta^{13}C$ remain apparent between species. This suggests that the isotopic composition of charcoal is established at relatively low temperatures in the production process. The data presented here indicates that the route by which charcoal aromatic structures are formed differs depending upon production variables and starting material, with a significant effect upon sample carbon isotopic values. These results have important implications both for understanding of the mechanisms by which plant $\delta^{13}C$ changes during charcoal formation, and for the use of charcoal $\delta^{13}C$ in palaeoenvironmental reconstruction.

Acknowledgements Funding for this work was provided by NERC standard grant NE/C004531/1 'Charcoal Degradation in Natural Environments'. The authors acknowledge Mike Cooper for TGA analysis at The University of Nottingham School of Chemical, Environmental and Mining Engineering, and the EPSRC solid state NMR service at Durham.

References

Alemany L. B., Grant D. M., Pugmuire R. J., Alger T. D. and Zilm K. W. (1983) Cross polarization and magic angle spinning NMR spectra of model compounds. II. Molecules of low or remote protonation. *J. Am. Chem. Soc*. **105**, 2142–2147.

Antal M. J. and Varhegyi G. (1995) Cellulose pyrolysis kinetics: The current state of knowledge. *Ind. Eng. Chem. Res*. **34**, 703 – 717.

Antal M. J., Allen S. G., Dai X. F., Shimizu B., Tam M. S., Gronli M. (2000) Attainment of the theoretical yield of carbon from biomass. *Industrial and Engineering Chemistry Research* **39**, 4024-4031.

Atalla R.H. and VanderHart D.L. (1999) The role of solid state ^{13}C NMR spectroscopy in studies of the structure of native celluloses. *Solid State Nucl. Magn. Reson.* **15**, 1-19.

Baldock J. A. and Smernik R. J. (2002) Chemical composition and bioavailability of thermally altered *Pinus resinosa* (Red pine) wood, *Organic Geochemistry* **33**, 1093–1109.

Benner R., Fogel M. F., Sprague E. K., and Hodson R. E. (1987). Depletion of ^{13}C in lignin and its implications for stable carbon isotope studies. *Nature* **329**, 708-710.

Beramendi-Orosco L., Snape C.E. and Large D.J. (2006). Stable carbon isotope analysis of wood hydropyrolysis residues: A potential indicator for the extent of cross-linking between lignin and polysaccharides, *Organic Geochemistry*, **37**, 64-71.

Bird M.I. and Gröcke D.R. (1997) Determination of the abundance and carbon isotope composition of elemental carbon in sediments. *Geochimica et Cosmochimica Acta* **61**, 3413–3423.

Blann W. G., Fyfe C. A., Lyerla J. R. and Yannoni C. S. (1981) High resolution ^{13}C NMR study of solid π-π molecular complexes using magic angle spinning techniques. *J. Am. Chem. Soc.* **103**, 4030-4033.

Cachier H,, Buat-Menard P. and Fontugne M. (1985). Source terms and source strengths of the carbonaceous aerosol in the tropics. *Journal of Atmospheric Chemistry* **3**, 469-489.

Carcaillet C., Almquist H., Asnong H., Bradshaw R. H. W., Carrión J. S., Gaillard M. –J., Gajewski K., Haas J. N., Haberle S. G., Hadorn P., Müller S. D., Richard P. J. H., Richoz I., Rösch M., Sánchez Goñi M. F., von Stedingk H., Stevenson A. C., Talon B., Tardy C., Tinner W., Tryterud E., Wick L. and Willis K. J. (2002). Holocene biomass burning and global dynamics of the carbon cycle. *Chemosphere*, **49**, 845-863.

Chaloner W. G. (1989). Fossil charcoal as an indicator of palaeoatmospheric oxygen level. *Journal of the Geological Society* **146**, 171-174.

Clark J. S., Grimm E. C., Lynch J. and Mueller P. G. (2001). Effects of Holocene climate change on the C4 grassland/woodland boundary in the Northern Plains, USA. *Ecology* **82**, 620-636.

Czimczik C. I,, Preston C. M., Schmidt M. W. I,. Werner R. A. and Schulze E-D. (2002). Effects of charring on mass, organic carbon and stable isotopic composition of wood. *Organic Geochemistry* **33**, 1207-1223.

Czimczik C. I., Schmidt M. W. I, and Schulze E.-D. (2005). Effects of increasing fire frequency on black carbon and organic matter in Podzols of Siberian Scots pine forests. *European Journal of Soil Science* **56**, 417–428.

Earl, W. L. and VanderHart, D. L. (1981) Observations by high-resolution carbon-13 nuclear magnetic resonance of cellulose I related to morphology and crystal structure. *Macromolecules* **14**, 570-574.

Eckmeier E., Gerlach R., Skjemstad J. O., Ehrmann O, and Schmidt M. W. I. (2007) Only small changes in soil organic carbon and charcoal found one year after experimental slash-and-burn in a temperate deciduous forest. *Biogeosciences Discuss.* **4**, 595-614.

Ehrlinger J. R., Cerling T. E. and Helliker B. R. (1997) C4 photosynthesis, atmospheric CO_2 and climate. *Oecologia* **112**, 285-299.

Ehrlinger J. R., Cerling T. E. and Dearing M. D. (2002) Atmospheric CO_2 as a Global Climate Change Driver Influencing Plant-Animal Interactions. *Integ. and Comp. Biol.* **42**, 424-430.

Evans R., Newman R.H., Roick U.C., Suckling I.D. and Wallis A.F.A. (1995) Changes in cellulose crystallinity during kraft pulping. Comparison of infrared, X-ray diffraction and solid state NMR results. *Holzforschung* **49**, 498-504.

Ferrio J. P., Araus J. L., Buxó R., Voltas J. and Bort J. (2005) Water management practices and climate in ancient agriculture: inference from the stable isotope composition of archaeobotanical remains. *Vegetation History and Archaeobotany* **14**, 510-517.

Fengel D. and Wegener G. (1984) Wood chemistry: Ultrastructure, reactions. Walter de Gruyter, New York.

Gavin D. G., Brubaker L. B. and Lertzman K. P. (2002) Holocene fire history of a coastal temperate rain forest based on soil charcoal radiocarbon dates. *Ecology* **84**, 186-201.

Gleixner G., Danier H. J., Werner R. A. and Schmidt H.-L. (1993) Correlations between the ^{13}C content of primary and secondary plant products in Different Cell Compartments and that in Decomposing Basidiomycetes. *Plant Physiology* **102**, 1287-1290.

Goebel T., Waters M. R. and Dikova M. (2003) The Archaeology of Ushki Lake, Kamchatka, and the Pleistocene Peopling of the Americas. *Science* **301**, 501-505.

Hall G., Woodborne S. and Scholes M. (2008) Stable carbon isotope ratios from archaeological charcoal as palaeoenvironmental indicators. *Chemical Geology* **247**, 384-400.

Hatcher P.G., Lerch, I., Harry, E., Bates, A.L. and Verheyen T.V. (1989) Solid-state ^{13}C nuclear magnetic resonance studies of coalified gymnosperm xylem tissue from Australian brown coals, *Organic Geochemistry* **14**, 145–155.

Hakkou M., Pétrissans M., Gérardin P. and Zoulalian A. (2006) Investigations of the reasons for fungal durability of heat-treated beech wood. *Polymer Degradation and Stability* **91**, 393-397.

Inari G. N., Mounguengui S., Dumarçay S., Pétrissans M. and Gérardin P. (2007) Evidence of char formation during wood heat treatment by mild pyrolysis. *Polymer Degradation and Stability* **92**, 997-1002.

Irbe, I., Andersone, I., Andersons, B., and Chirkova, J. (2001) Use of ^{13}C NMR, sorption and chemical analysis for characteristics of brown-rotted Scots pine, *International Biodeterioration and Biodegradation* **47**, 37–45.

Jones T.P, Scott A.C. and Mattey D.P. (1993) Investigations of "fusian transition fossils" from the Lower Carboniferous: comparisons with modern partially charred wood. *International Journal of Coal Geology* **22**, 37–59.

Knicker H., Almendros G., González-Vila F. J., Martin F. and Lüdemann H.-D. (1996) ^{13}C- and ^{15}N- NMR spectroscopic examination of the transformation of organic nitrogen in plant biomass during thermal treatment. *Soil Biology and Biochemistry* **28**, 1053-1060.

Kringstad K. P. and Mörck R. (1983) ^{13}C-NMR spectra of kraft. lignins. *Holzforschung* **37**, 237–244.

Krull E. S., Skjemstad J. O., Graetz D., Grice K., Dunning W., Cook G. and Parr J. F. (2003) ^{13}C-depleted charcoal from C4 grasses and the role of occluded carbon in phytoliths. *Organic Geochemistry* **34**, 1337-1352.

Labbé N., Harper D., Rials T. and Elder T. (2006) Chemical Structure of Wood Charcoal by Infrared Spectroscopy and Multivariate analysis. *Journal of Agricultural and Food Chemistry* **54**, 3492-3497.

5.1

Leavitt S.W. and Long A. (1984) Sampling strategy for stable carbon isotope analysis of tree rings in pine. *Nature* **311**, 145–147.

Levine J. S. (1991). Global Biomass Burning: Atmospheric, Climatic and Biospheric Implications. MIT Press, Cambridge, Massachusetts.

Loader N.J., Robertson I. and McCarroll D. (2003) Comparison of stable carbon isotope ratios in the whole wood, cellulose and. lignin of oak tree-rings. *Palaeogeogr. Palaeoclimatol. Palaeoecol.* **196**, 395–407.

Li J., Li B. and Zhang X. (2002) Comparative studies of thermal degradation between larch lignin and manchurian ash lignin. *Polymer degradation and stability* **78**, 279-285.

Marino B.D. and DeNiro M.J. (1987) Isotopic analysis of archaeobotanicals to reconstruct past climates: Effects of activities associated with food preparation on carbon, hydrogen and oxygen isotope ratios of plant cellulose. *Journal of Archaeological Science* **14**, 537–548.

Martinez A. T., Almendros G., Gonzalez-Vila F.-J. and Frund R. (1999) Solid-state spectroscopic analysis of lignins from several Austral hardwoods. *Solid State Nucl Mag Resonance* **15**, 41-48.

Maunu S.L. (2002) NMR studies of wood and wood products. Prog Nuci Magn Reson Spectrosc **40**, 151-174.

McCarroll D. and Loader N. J. (2004) Stable Isotopes in Tree Rings. *Quaternary Science Reviews* **23**, 771-801.

Mok W. S. L., Antal M. J., Szabo P., Varhegyi G. and Zelei B. (1992) Formation of Charcoal from Biomass in a Sealed Reactor. *Industrial and Engineering Chemistry Research* **31**, 1162-1166.

Mörck R. and Kringstad K. P. (1985) ^{13}C-NMR Spectra of Kraft lignins. *Holzforschung* **39**, 109–119.

Nogueira M. C. J. A., Tavares M. I. B. and Nogueira J. S. (2004). ^{13}C NMR Molecular dynamic investigation of tropical wood Angelin Pedra (Hymenolobium paetrum). *Polymer* **45**, 1217-1222.

Novakov T., Cachier H., Clark J. S., Gaudichet A., Macko S. and Masclet P. (1994). Characterization of particulate products of biomass combustion. In *Sediment records of biomass burning and global change* (eds. Clark J. S, Cachier H, Goldammer H. G, and Stocks B. J.) Springer-Verlag, Berlin, Germany. Pp 117-143.

Pandey K. K. 1998. A study of chemical structure of soft and hardwood and wood polymers by FTIR spectroscopy. *Journal of Applied Polymer Science* **71**, 1969-1975.

Poole I., Braadbaart F., Boon J. J. and van Bergen P. F. (2002). Stable carbon isotopic changes during artificial charring of propagules. *Organic geochemistry* **33** 1675-1681.

Pessenda L. C. R., Ledru M. P., Gouveia S. E.M. N., Aravena R., Ribeiro A. S., Bendashsollil J. A. and Boulet R. (2005) Holocene palaeoenvironmental reconstruction in north eastern Brazil inferred from pollen, charcoal and carbon isotope records. *The Holocene* **15**, 812-820.

Preston C.M. 2001. Carbon-13 solid-state NMR of soil organic matter—using the technique effectively. *Canadian. Journal of Soil Science* **81**, 255–270.

Qian Y., Engel M.H. and Macko S.A. 1992. Stable isotope fractionation of biomonomers during protokerogen formation. *Chemical Geology* **101**, 201–210.

Robertson, I.; Switsur, V. R.; Carter, A. H. C.; Barker, A. C.; Waterhouse, J. S.; Briffa, K. R.; Jones, P. D. 1997. Signal strength and climate relationships in $^{13}C/^{12}C$ ratios of tree ring cellulose from oak in east England. Journal of Geophysical Research, Volume 102, Issue D16, p. 19507-19516.

Richard J.-R. and Antal, M. J. (1994) Thermogravimetric Studies of Charcoal Formatiom from Cellulose at. Elevated Pressures. In *Advances in Thermochemical Biomass Conversion* (ed. Bridgwater, A. V.) Blackie Academic & Professional, London. Pp 784-792.

Sima-Ella E., Yuan G. and Mays T. (2005) A simple kinetic analysis to determine the intrinsic reactivity of coal char. *Fuel* **84**, 1920–1925.

Simpson M. J. and Hatcher P. G. (2004) Overestimates of black carbon in soils and sediments. *Naturwissenschaften* **91**, 436–440.

Sivonen H., Maunu S.L., Sundholm F., Jämsä S. and Viitaniemi P. (2002) Magnetic resonance studies of thermally modified wood. *Holzforschung* **56** , 648–654.

Sjöström E. (1993) *Wood chemistry. Fundamentals and applications*. Academic Press Inc, London, UK. pp. 140–164.

Skjemstad J. O., Clarke P., Taylor J. A., Oades J. M. and McClure S. G. (1996) The Chemistry and Nature of Protected Carbon in Soil. *Australian Journal of Soil Research*. **34**, 251-276.

Skjemstad J. O,, Reicosky D. C., Wilts A. R. and McGowan J. A. (2002) Charcoal Carbon in US Agricultural Soils. *Soil Sci. Soc. Am. J.* **66**, 1249-1255.

Soares S., Ricardo N. M. P. S., Jones S. and Heatley F. (2001) High temperature thermal degradation of cellulose in air studied using FTIR and ^{1}H and ^{13}C solid-state NMR. *European polymer journal* **37**, 737-745.

Steinbeiss, S., Schmidt, C.M., Heide, K. and Gleixner, G. (2006) $\delta^{13}C$ values of pyrolysis products from cellulose and lignin represent the isotope content of their precursors, *Journal of Analytical and Applied Pyrolysis* **75**, 19–26.

Swift, L.W. Jr., Elliott, KJ., Ottmar, R.D., and Vihnanek, R.E. (1993) Site preparation burning to improve southern Appalachian pine-hardwood stands: fire characteristics and soil erosion, moisture, and temperature. *Canadian Journal of Forest Research* **23,** 2242-2254.

Turekian V. C., Macko S., Ballantine D., Swap R. J. and Garstang M. (1998). Causes of bulk carbon and nitrogen isotopic fractionations in the products of vegetation burns: laboratory studies. *Chemical Geology* **152**, 181-192.

Turney C.S.M., Wheeler D. and Chivas A.R. (2006) Carbon isotope fractionation in wood during carbonization, *Geochimica et Cosmochimica Acta* **70**, 960–964.

Verheyden A., Roggeman, M., Bouillon, S., Elskens, M., Beeckman, H. and Koedam, N. (2005) Comparison between $\delta^{13}C$ of a-cellulose and bulk wood in the mangrove tree *Rhizophora mucronata*: implications for dendrochemistry. *Chemical Geology.* **219**, 275-282.

Völker S. and Rieckmann T. (2002) Thermokinetic investigation of cellulose pyrolysis - impact of initial and final mass on kinetic results. *Journal of Analytical and Applied Pyrolysis* **62**, 165-177.

Werts S. P. and Jahren A. H. (2007) Estimation of temperatures beneath archaeological campfires using stable isotopic composition of soil organic matter. *Journal of Archaeological Science* **34**, 850-857.

Wikberg H. and Maunu S. L. (2004). Characterization of thermally modified hard- and softwoods by ^{13}C CPMAS NMR. *Carbohydrate polymers* **58**, 461-466.

Williams P. T. and Besler S. (1996). The influence of temperature and heating rate on the slow pyrolysis of biomass. *Renewable Energy* **7**, 233-250.

Wilson A.T. and Grinstead M.J. (1977) $^{12}C/^{13}C$ in cellulose and lignin as palaethermometers. *Nature* **265**, 133-135.

Wormald, P., Wickholm K., Larsson P.T. and Iversen T. (1996). Conversions between ordered and disordered cellulose. Effects of mechanical treatment followed by cyclic wetting and drying. *Cellulose* **3**, 141-152.

Xiao B., Sun X. F. and Sun R. 2001. Chemical, structural, and thermal characterizations of alkali-soluble lignins and hemicelluloses, and cellulose from maize stems, rye straw, and rice straw. *Polymer Degradation and Stability* **74**, 307-319.

Tables

Table 1: Measured values for %C and $\delta^{13}C$ of pine and mangrove wood samples and extracted lipids from samples prior to pyrolysis.

Wood material	**%C**	**$\delta^{13}C$**
Pine	47.19	-26.67
Pine lipids	63.00	-28.24
Mangrove	45.05	-28.04
Mangrove lipids	48.30	-32.27

Table 2: Weight loss and moisture content of samples on charring under various pyrolysis conditions. Measurement precision was better than ±0.5% (1σ).
*Insufficient sample for analysis

			1 cm^3 cube				1-2mm chip			
			Pine		Mangrove		Pine		Mangrove	
Time (min)	**T (°C)**	**%O_2**	**% wt loss (g)**	**% H_2O**	**% wt loss (g)**	**% H_2O**	**% wt loss (g)**	**% H_2O**	**% wt loss (g)**	**% H_2O**
60	**300**	0	55.31	4.9	54.74	4.1	65.94	4.0	64.39	4.1
60	**400**	0	75.73	4.3	65.26	4.4	76.35	4.7	65.26	2.5
60	**500**	0	78.99	3.5	68.92	5.0	79.78	3.8	75.63	4.9
60	**600**	0	80.41	4.3	71.35	4.4	82.45	4.4	78.76	5.7
120	**300**	0	69.09	2.7	59.18	3.9	69.85	2.6	63.89	2.0
120	**400**	0	75.86	4.3	65.65	4.9	77.36	4.2	76.89	4.6
120	**500**	0	79.29	5.2	68.63	3.7	81.13	4.7	80.87	4.6
120	**600**	0	80.89	6.3	71.62	6.1	81.25	5.8	78.56	6.5
60	**300**	2	63.62	3.2	50.24	1.8	72.57	5.6	60.03	4.9
60	**400**	2	78.41	6.8	69.31	3.0	81.92	6.2	86.69	10.6
60	**500**	2	87.53	8.2	78.25	2.1	92.47	11.8	98.14	*
60	**600**	2	91.44	7.8	80.69	2.0	96.91	6.1	98.92	*
120	**300**	2	66.17	8.1	53.18	1.7	72.49	6.6	64.34	3.9
120	**400**	2	85.33	10.7	74.96	9.7	86.32	11.3	96.67	*
120	**500**	2	94.59	10.7	89.29	6.1	99.47	25.6	99.30	*
120	**600**	2	97.19	9.6	91.68	8.9	99.86	*	98.85	*

Table 3: %C and Δ%C (change with respect to raw wood where pine = 47.19% and mangrove = 45.05%) of samples after exposure to various production conditions. Measurement precision was better than ±0.3% (1σ).
*Insufficient sample for analysis

			1 cm^3 Cube				1-2mm Chip			
Production conditions			**Pine**		**Mangrove**		**Pine**		**Mangrove**	
Time (min)	**T (°C)**	**%O_2**	**%C**	**Δ%C**	**%C**	**Δ%C**	**% C**	**Δ%C**	**%C**	**Δ%C**
60	**300**	0	63.64	16.45	69.59	24.54	68.09	20.90	69.24	24.19
60	**400**	0	75.51	28.32	73.97	28.92	74.39	27.20	76.52	31.47
60	**500**	0	82.71	35.52	83.61	38.56	81.47	34.28	81.50	36.45
60	**600**	0	86.63	39.44	84.76	39.71	85.58	38.39	84.56	39.51
120	**300**	0	69.53	22.34	68.44	23.39	69.57	22.38	71.32	26.27
120	**400**	0	75.39	28.20	78.28	33.23	76.08	28.89	76.48	31.43
120	**500**	0	83.25	36.06	85.33	40.28	84.75	37.56	82.27	37.22
120	**600**	0	85.99	38.80	85.72	40.67	83.63	36.44	83.94	38.89
60	**300**	2	68.19	21.00	67.37	22.32	65.72	18.53	66.47	21.42
60	**400**	2	70.50	23.31	73.16	28.11	72.70	25.51	71.12	26.07
60	**500**	2	78.92	31.73	83.77	38.72	71.79	24.60	82.46	37.41
60	**600**	2	88.31	41.12	87.97	42.92	87.43	40.24	*	*
120	**300**	2	64.22	17.03	70.23	25.18	66.29	19.10	66.36	21.31
120	**400**	2	65.57	18.38	72.11	27.06	68.53	21.34	69.89	24.84
120	**500**	2	80.66	33.47	84.59	39.54	72.19	25.00	*	*
120	**600**	2	88.47	41.28	86.87	41.82	85.59	38.40	*	*

Table 4: $\delta^{13}C$ and $\Delta\ \delta^{13}C$ (change with respect to raw wood where pine = -26.67‰ and mangrove = -28.04‰) of samples after exposure to various conditions. Measurement precision was better than ±0.2‰ (1σ).
*Insufficient sample for analysis
***Single measurements due to sample size

			1 cm^3 Cube				**1-2mm Chip**			
Production conditions			**Pine**		**Mangrove**		**Pine**		**Mangrove**	
Time (min)	**T (ºC)**	**%O_2**	**$\delta^{13}C$**	**$\Delta\ \delta^{13}C$**	**$\delta^{13}C$**	**$\Delta\ \delta^{13}C$**	**$\delta^{13}C$**	**$\Delta\ \delta^{13}C$**	**$\delta^{13}C$**	**$\Delta\ \delta^{13}C$**
60	**300**	0	-27.19	-0.52	-27.61	0.43	-27.87	-1.20	-28.18	-0.14
60	**400**	0	-27.59	-0.92	-28.31	-0.27	-27.36	-0.69	-28.75	-0.71
60	**500**	0	-27.91	-1.24	-28.72	-0.68	-27.87	-1.20	-28.68	-0.64
60	**600**	0	-27.86	-1.19	-28.63	-0.59	-27.84	-1.17	-28.68	-0.64
120	**300**	0	-27.62	-0.95	-28.21	-0.17	-27.20	-0.53	-28.28	-0.24
120	**400**	0	-27.69	-1.02	-28.53	-0.49	-28.16	-1.49	-28.50	-0.46
120	**500**	0	-26.92	-0.25	-28.44	-0.40	-27.52	-0.85	-28.48	-0.44
120	**600**	0	-27.71	-1.04	-28.36	-0.32	-28.13	-1.46	-28.81	-0.77
60	**300**	2	-27.33	-0.66	-27.49	0.55	-27.37	-0.70	-28.06	-0.02
60	**400**	2	-27.60	-0.93	-28.11	-0.07	-27.46	-0.79	-28.06	-0.02
60	**500**	2	-27.86	-1.19	-28.41	-0.37	-27.48	-0.81	-28.37	-0.33
60	**600**	2	-28.25	-1.58	-28.37	-0.33	-28.10	-1.43	*	*
120	**300**	2	-27.23	-0.56	-27.96	0.08	-27.27	-0.60	-28.19	-0.15
120	**400**	2	-27.43	-0.76	-28.14	-0.10	-27.24	-0.57	-27.84	0.20
120	**500**	2	-27.76	-1.09	-28.59	-0.55	-27.08	-0.41	-27.97***	0.07
120	**600**	2	-27.50	-0.83	-27.88	0.16	-27.96	-1.29	-28.26***	-0.22

Table 5: Proportion of aliphatic and aromatic C (relative intensity [% total area]) in ^{13}C-CP-SSNMR spectra in the structural composition of pine (*Pinus sylvestris* L) and mangrove (*Rhizophora apiculata* Blume) wood, and charcoal prepared from both species under two gas compositions and at temperatures between 300°C-600°C.

Production conditions		**Pine**		**Mangrove**	
T (°C)	**%O_2**	**% Aliphatic**	**% Aromatic**	**Aliphatic**	**Aromatic**
-	-	88.15	11.85	82.21	17.79
300	0	51.88	48.13	42.53	57.47
400	0	9.20	90.80	19.06	80.94
500	0	0.00	100.00	0.00	100.00
600	0	5.67	94.33	0.00	100.00
300	2	35.90	64.10	49.71	50.29
400	2	14.41	85.59	5.74	94.26
500	2	0.00	100.00	0.90	99.10
600	2	0.00	100.00	0.00	100.00

Figure captions

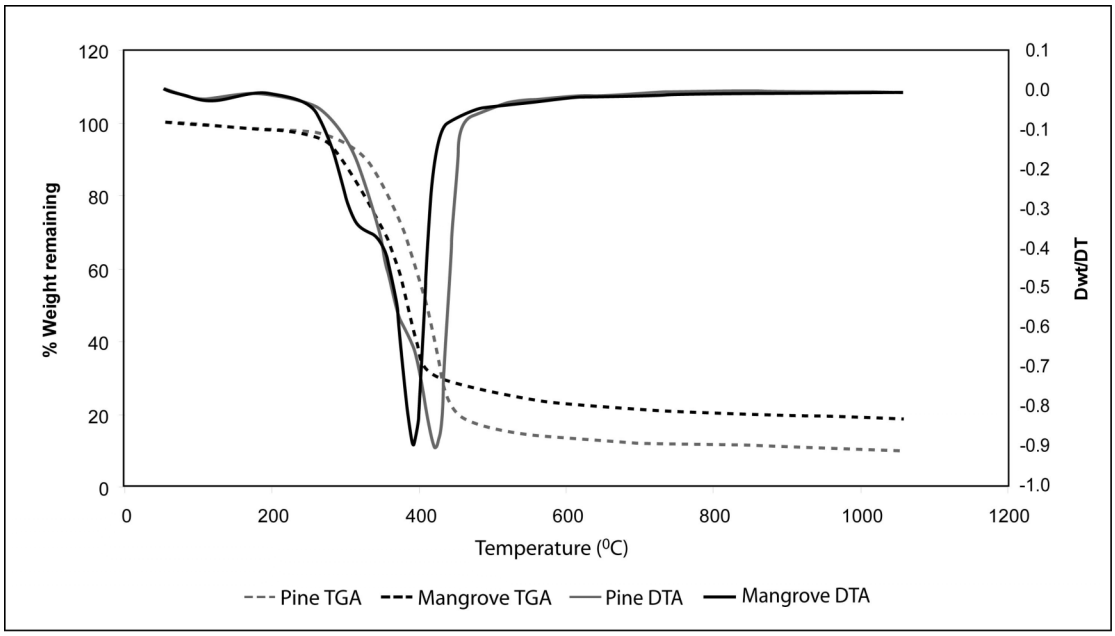

Figure 1: Ascough *et al.*

Figure 1: Experimental mass loss curves (dashed lines), and evolution of the mass loss rate (solid lines) for proximate TGA analysis of untreated pine and mangrove wood in an inert (N_2) atmosphere for the interval 25-1000ºC.

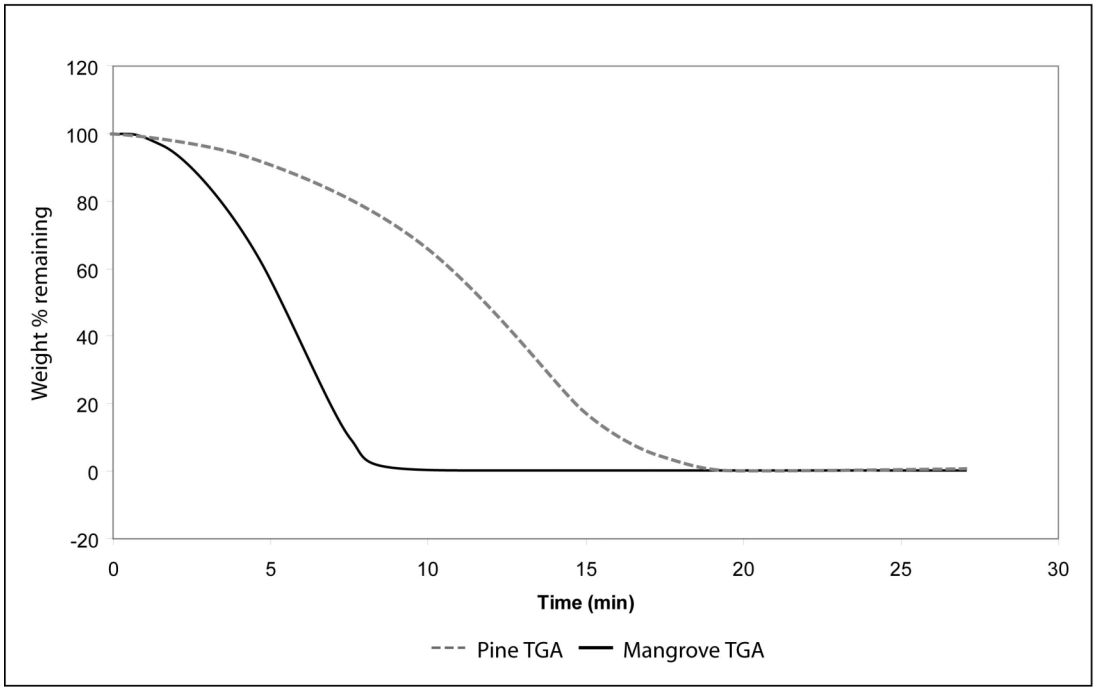

Figure 2: Ascough *et al.*

Figure 2: Isothermal TGA analysis of devolatilized pine (grey dashed line) and mangrove (solid black line) charcoal in an oxidizing (air) atmosphere at 525ºC.

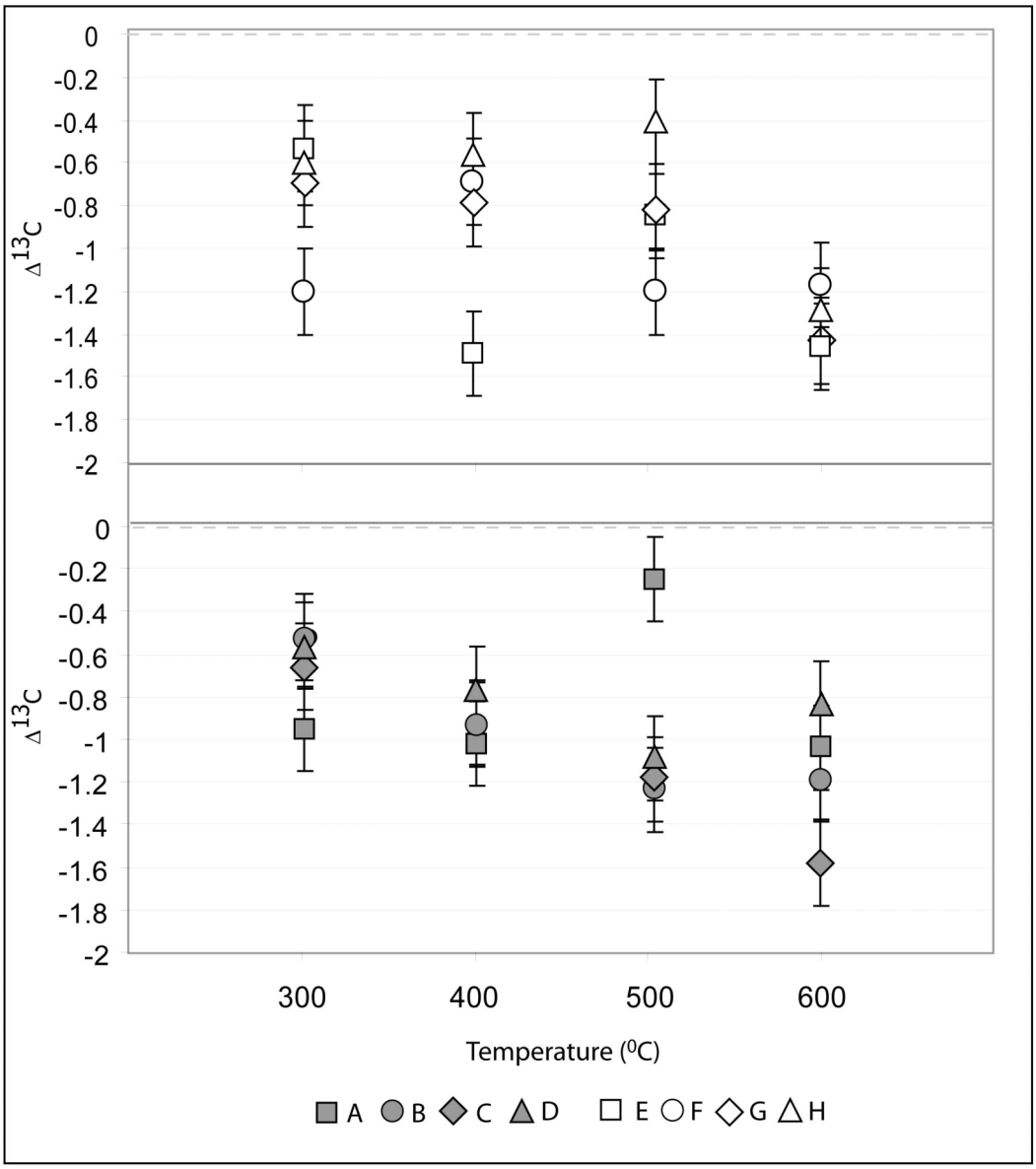

Figure 3 Ascough *et al.*

Figure 3: Change in $\delta^{13}C$ of pine charcoal with respect to untreated wood ($\Delta^{13}C$) at temperatures of 300-600ºC. Pine 1cm^3 cubes pyrolysed in N_2 for 60 min (A), 120 min (B) and in 2% O_2 for 60 min (C), 120 min (D). Pine 1-2mm chips pyrolysed in N_2 for 60 min (E), 120 min (F) and in 2% O_2 for 60 min (G), 120 min (H).

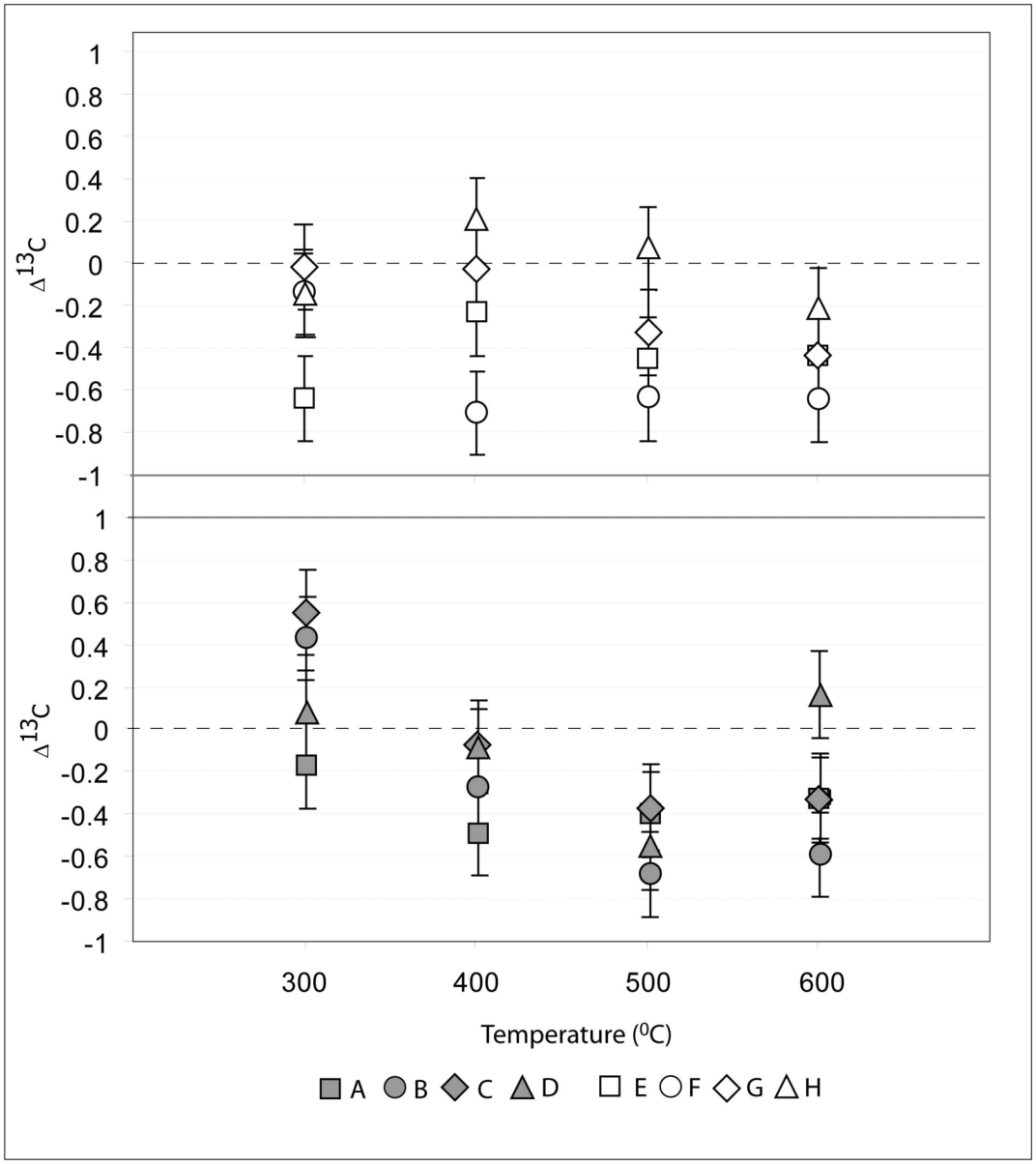

Figure 4: Ascough *et al.*

Figure 4: Change in $\delta^{13}C$ of mangrove charcoal with respect to untreated wood ($\Delta^{13}C$) at temperatures of 300-600ºC. Mangrove 1cm^3 cubes pyrolysed in N_2 for 60 min (A), 120 min (B) and in 2% O_2 for 60 min (C), 120 min (D). Mangrove 1-2mm chips pyrolysed in N_2 for 60 min (E), 120 min (F) and in 2% O_2 for 60 min (G), 120 min (H).

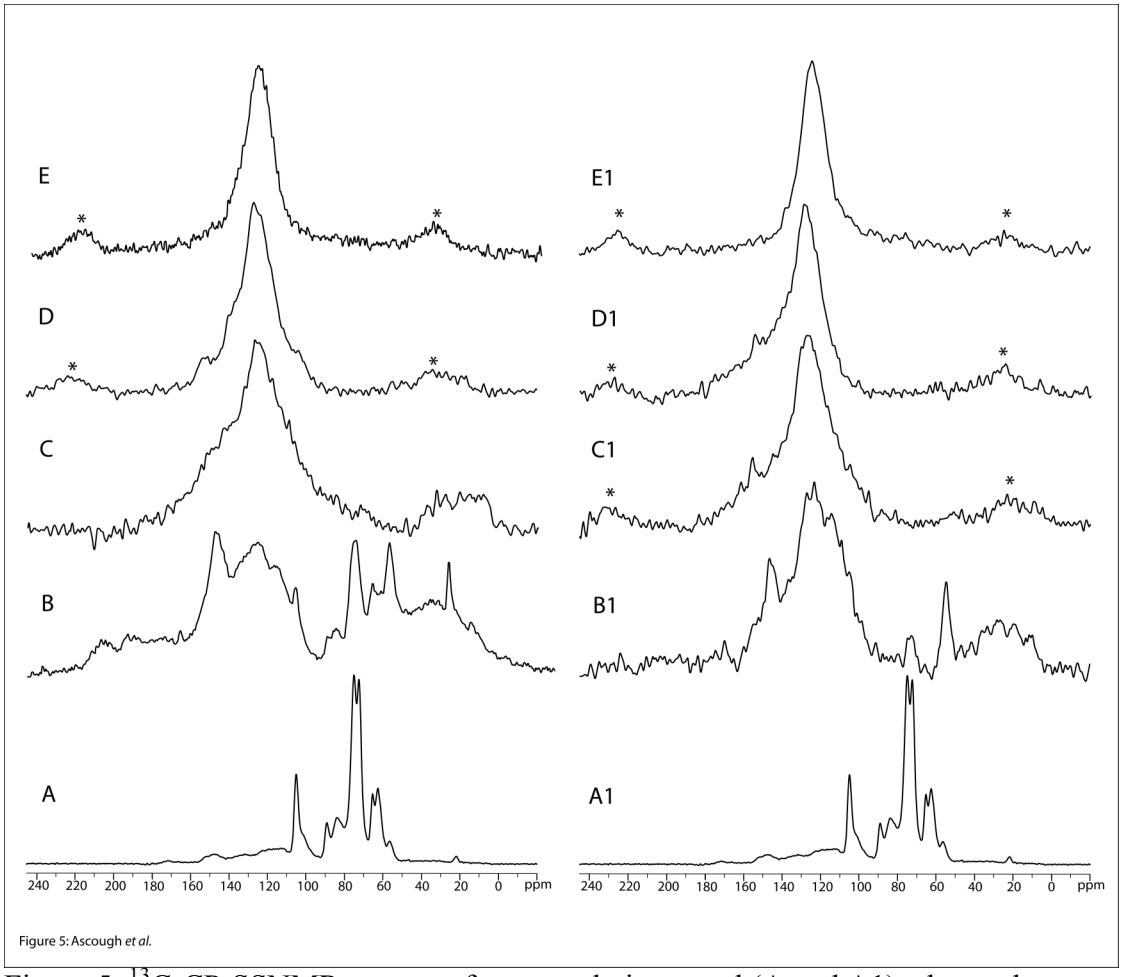

Figure 5: ^{13}C-CP-SSNMR spectra of untreated pine wood (A and A1), charcoal prepared from pine by heating in N_2 at 300ºC (B), 400ºC (C), 500ºC (D), and 600ºC (E), and charcoal prepared from pine by heating in 2% O_2 at 300ºC (B1), 400ºC (C1), 500ºC (D1), and 600ºC (E1). Spinning side bands are indicated by *.

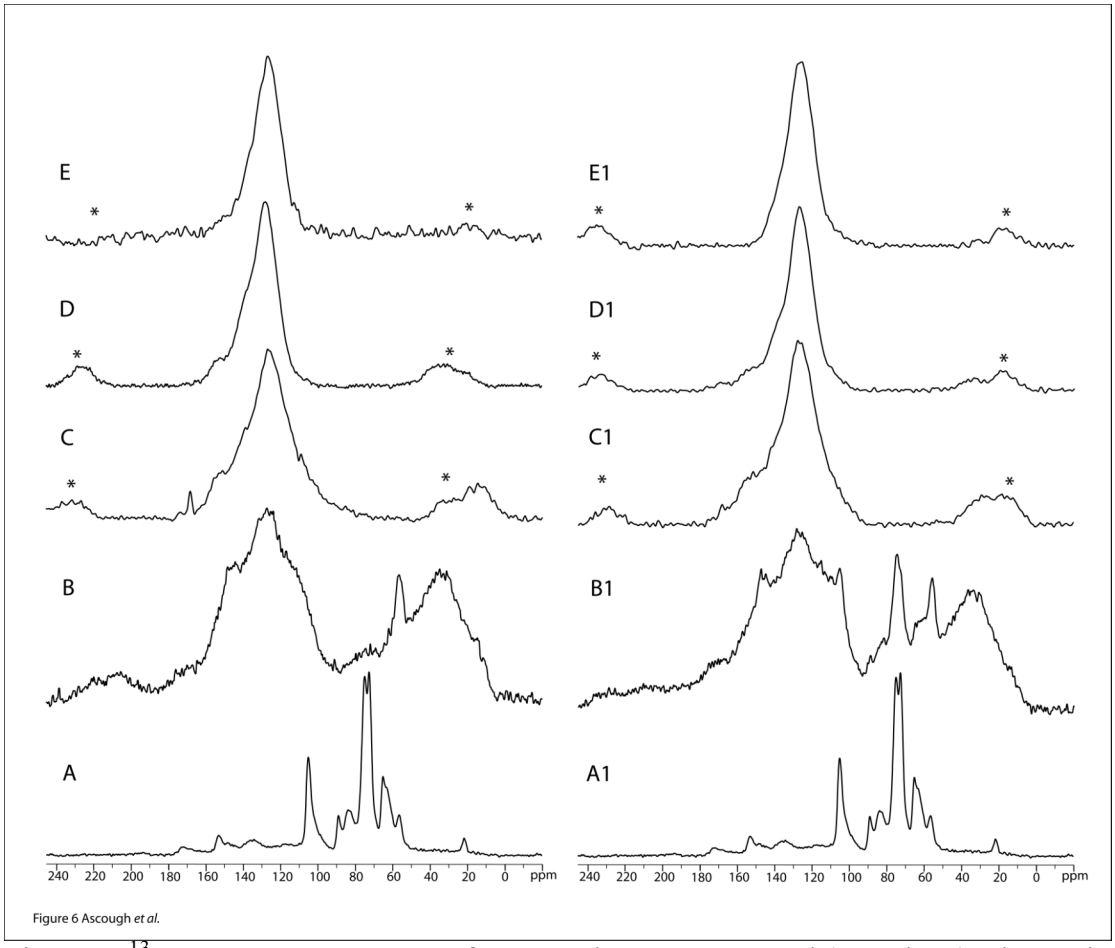

Figure 6: ^{13}C-CP-SSNMR spectra of untreated mangrove wood (A and A1), charcoal prepared from mangrove by heating in N_2 at 300ºC (B), 400ºC (C), 500ºC (D), and 600ºC (E), and charcoal prepared from mangrove by heating in 2% O_2 at 300ºC (B1), 400ºC (C1), 500ºC (D1), and 600ºC (E1). Spinning side bands are indicated by *.

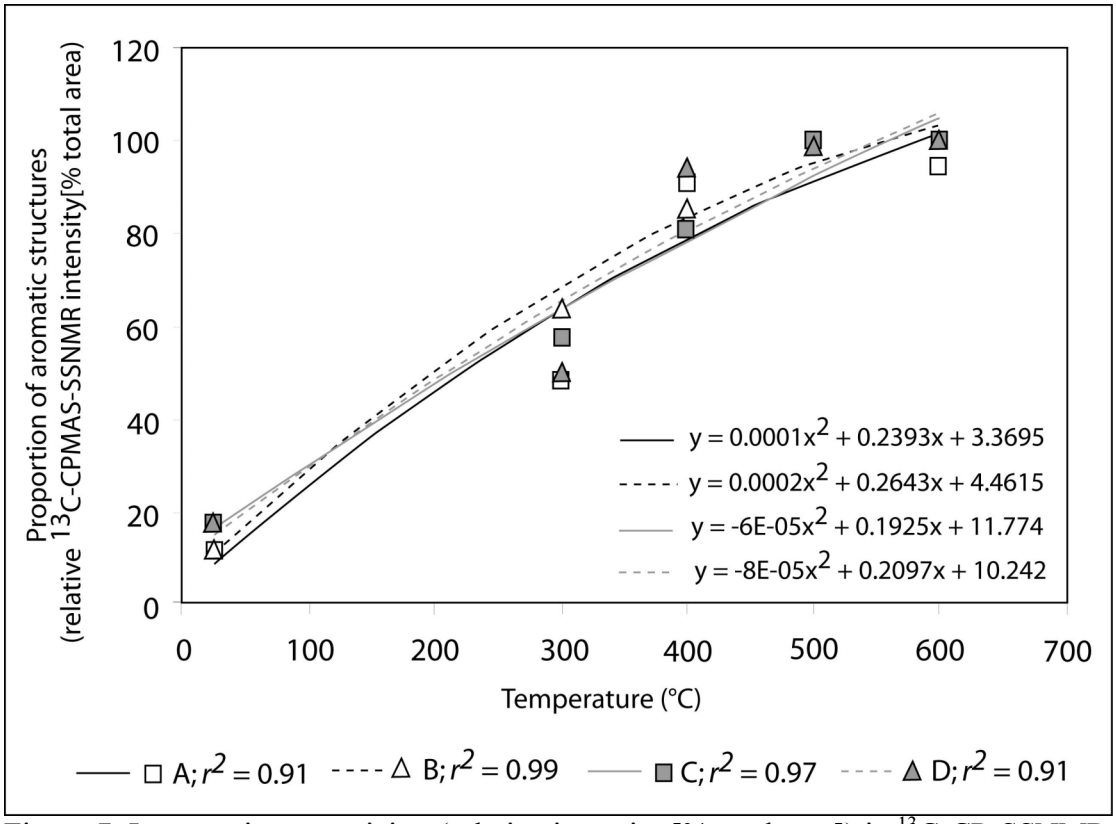

Figure 7: Increase in aromaticity, (relative intensity [% total area]) in ^{13}C-CP-SSNMR spectra with change in production temperature in charcoal prepared from (A) pine wood under N_2, (B) pine wood under 2% O_2, (C) mangrove wood under N_2, (D) mangrove wood under 2% O_2. r^2 values for a second-order polynomial are better than 0.9 (P = <0.05) for all sample types.

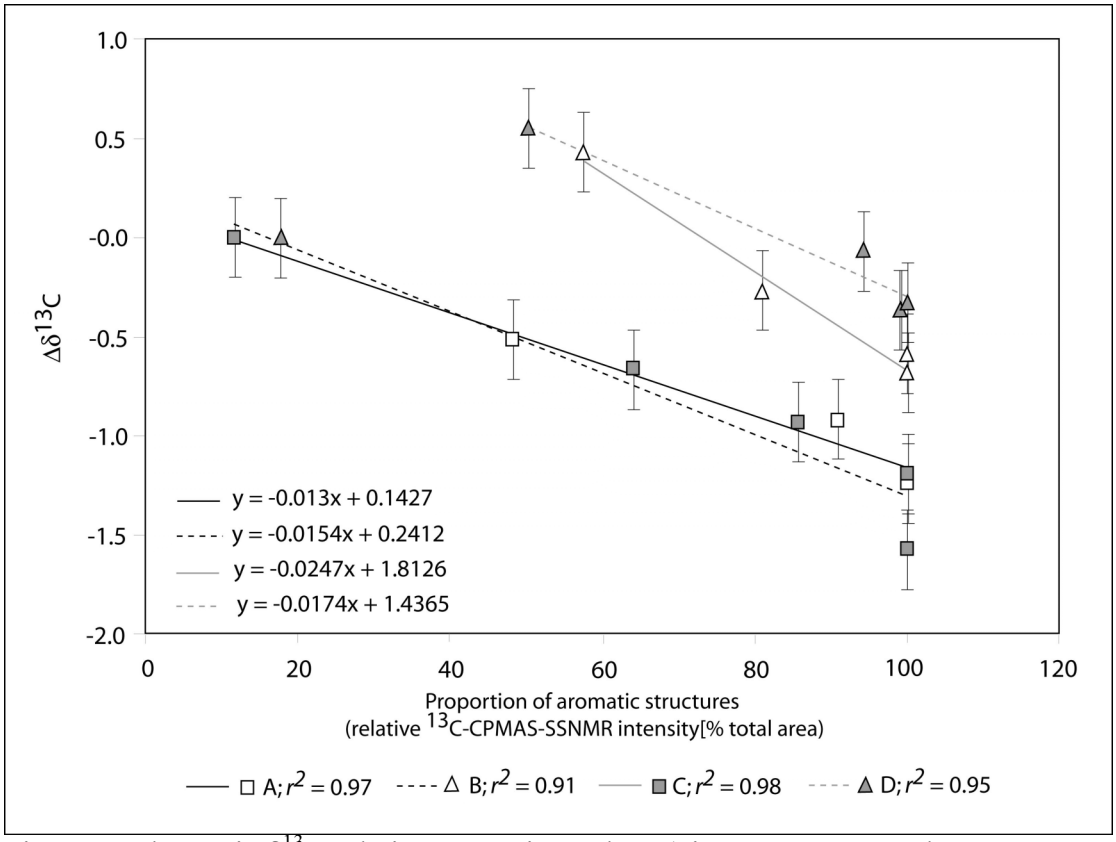

Figure 8: Change in $\delta^{13}C$ relative to starting values (pine = -26.67‰ and mangrove = -28.04‰) with increasing aromaticity (relative intensity [% total area]) in ^{13}C-CP-SSNMR spectra in charcoal prepared from (A) pine wood under N_2, (B) pine wood under 2% O_2, (C) mangrove wood under N_2, (D) mangrove wood under 2% O_2. r^2 values for a linear correlation are better than 0.9 (P = <0.05) for all pine samples, and for mangrove samples after 300°C.